

## Article

# Characterization of Two Hydrogen Peroxide Resistant Peroxidases from *Rhodococcus opacus* 1CP

Anna Christina R. Ngo<sup>1</sup>, Catleen Conrad<sup>2,3</sup>, Álvaro Gómez Baraibar<sup>1</sup> , Anke Matura<sup>3</sup>, Karl-Heinz van Pée<sup>3</sup> and Dirk Tischler<sup>1,2,\*</sup> 

<sup>1</sup> Microbial Biotechnology, Ruhr University Bochum, Universitätsstraße 150, 44780 Bochum, Germany; Anna.Ngo@rub.de (A.C.R.N.); Alvaro.Baraibar@rub.de (Á.G.B.)

<sup>2</sup> Institute of Biosciences, Environmental Microbiology, TU Bergakademie Freiberg, Leipziger Str. 29, 09599 Freiberg, Germany; catleen.conrad@gmx.de

<sup>3</sup> Allgemeine Biochemie, Technische Universität Dresden, 01062 Dresden, Germany; Anke.Matura@chemie.tu-dresden.de (A.M.); Karl-Heinz.vanPee@chemie.tu-dresden.de (K.-H.v.P.)

\* Correspondence: dirk.tischler@rub.de; Tel.: +49-234-32-22656

**Abstract:** The dye-decolorizing peroxidases (DyP) are a family of heme-dependent enzymes present on a broad spectrum of microorganisms. While the natural function of these enzymes is not fully understood, their capacity to degrade highly contaminant pigments such as azo dyes or anthraquinones make them excellent candidates for applications in bioremediation and organic synthesis. In this work, two novel DyP peroxidases from the organism *Rhodococcus opacus* 1CP (DypA and DypB) were cloned and expressed in *Escherichia coli*. The enzymes were purified and biochemically characterized. The activities of the two DyPs via 2,2'-azino-bis [3-ethylbenzthiazoline-6-sulphonic acid] (ABTS) assay and against Reactive Blue 5 were assessed and optimized. Results showed varying trends for DypA and DypB. Remarkably, these enzymes presented a particularly high tolerance towards H<sub>2</sub>O<sub>2</sub>, retaining its activities at about 10 mM H<sub>2</sub>O<sub>2</sub> for DypA and about 4.9 mM H<sub>2</sub>O<sub>2</sub> for DypB.

**Keywords:** Dyp-type peroxidase; heme-dependent enzyme; dye degradation; biotransformation; Actionbacteria; H<sub>2</sub>O<sub>2</sub> tolerance



**Citation:** Ngo, A.C.R.; Conrad, C.; Gómez Baraibar, Á.; Matura, A.; van Pée, K.-H.; Tischler, D.

Characterization of Two Hydrogen Peroxide Resistant Peroxidases from *Rhodococcus opacus* 1CP. *Appl. Sci.* **2021**, *11*, 7941. <https://doi.org/10.3390/app11177941>

Academic Editors: Giorgia Spigno and Paola Grenni

Received: 30 June 2021

Accepted: 26 August 2021

Published: 27 August 2021

**Publisher's Note:** MDPI stays neutral with regard to jurisdictional claims in published maps and institutional affiliations.



**Copyright:** © 2021 by the authors. Licensee MDPI, Basel, Switzerland. This article is an open access article distributed under the terms and conditions of the Creative Commons Attribution (CC BY) license (<https://creativecommons.org/licenses/by/4.0/>).

## 1. Introduction

Different industries are now gearing towards greener solutions—phasing out traditional chemical processes that are often found to be harmful to human and the environment. In search of finding other alternatives, enzymes have been used as a potential agent to drive these sustainable processes as they are more environmental-friendly, non-toxic, and more cost-efficient in the long run [1–3]. A particularly interesting family of enzymes that are being used for industrial applications are the dye-decolorizing peroxidases (DyPs) (EC 1.11.1.19), which can oxidize recalcitrant organic compounds using hydrogen peroxide (H<sub>2</sub>O<sub>2</sub>) as co-substrate [4–8]. This enzyme can degrade different types of dyes, which can make them extremely useful in the treatment of wastewater produced by the textile industry or as decolorizing agents in the cosmetics or food industry [9,10]. Another potential use for these proteins is the valorization of lignin since they are one of the few enzymes able to degrade this natural polymer [11]. Due to the wide availability of lignin, its chemical variety, and its resistance to treatment, the DyPs offer a great potential alternative for the field of synthetic green chemistry [12–15].

Nevertheless, in the search for an application, two main hurdles have been identified for this type of enzyme: their sensitivity to the H<sub>2</sub>O<sub>2</sub> that they require to operate and the difficulty of heterologous expression [16].

Since the peroxide sensitivity is an issue presented by many different heme-containing proteins [17,18], strategies like the combination with oxidases for in situ production of H<sub>2</sub>O<sub>2</sub> have been attempted [19]. Another option has been the modification of the enzyme to

increase its stability towards its substrate since it is generally considered that the presence of sensitive amino acids close to the heme group is responsible for the peroxide inactivation. In the DypB of *Rhodococcus jostii*, mutations to the Asp153 have been shown to have a beneficial effect in this parameter [20]. Another example was the introduction of the T134V and M212L mutations in the PpDyp from *Pseudomonas putida* [21].

Meanwhile, the difficulty of heterologous expression posed a challenge earlier since the first DyPs characterized were found in fungi. They tend to present high levels of glycosylation making it difficult to express in organisms like *Escherichia coli*. This issue was overcome after the discovery and subsequent heterologous expression of bacterial DyPs. To date, several bacterial DyPs have been described in many different organisms such as cyanobacteria [22], bacillus [23], actinomycetes such as *Thermobifida fusca* [24–26], *Amycolatopsis* [27], *Rhodococcus jostii* [28–30], *Saccharomonospora viridis* [31] and Gammaproteobacteria such as different species of *Pseudomonas* [32–34] or *E. coli* [35]. Strategies to improve protein production in *E. coli* such as the addition of hemin still needs to be explored on since it does not incorporate heme properly. Despite the growing data on these bacterial peroxidases, optimizing protein production is still needed to be explored on.

Actinobacteria is a phylum well-known for their capacity to degrade organic pollutants. Several research studies have already shown the applicability of actinobacteria such as *Corynebacterium* sp. [36], *Streptomyces* sp. [37], and *Rhodococcus* sp. [38] to name a few. *Rhodococcus* sp. has been a subject of interest in different biotechnological applications due to the promising enzymes it harbors. *Rhodococcus opacus* has been a subject of biotechnological interest for its capacity to produce fatty acids [39,40]. Moreover, it is capable of utilizing several different carbon sources as well as its stability towards different organic solvents makes it an extremely interesting option for industrial applications [41,42]. Many interesting xenobiotic-degrading enzymes have already been characterized such as styrene monooxygenases [43], styrene oxide isomerases [44], phenol hydroxylases [45], azobenzene reductases [46], and among others. Despite the myriad of enzymes found and studied on *R. opacus* 1CP, the dye decolorizing peroxidases, DypA and DypB, are not established yet.

Therefore, the study aimed to clone, express, purify, and characterize the biochemical properties of DypA and DypB. Their tolerance towards H<sub>2</sub>O<sub>2</sub> and their potential to degrade dyes of different structures was also investigated. In addition, deeper insights into its mechanism towards Reactive Blue 5 were done.

## 2. Materials and Methods

### 2.1. Chemicals and Culture Conditions

The strain *Rhodococcus opacus* 1CP was the donator of the DyP genes. All chemicals were purchased from MERCK (Darmstadt, Germany), VWR (Dresden, Germany), Sigma-Aldrich (Taufkirchen, Germany), AppliChem (Darmstadt, Germany), Grüssing (Filsium, Germany), and Difco (Fisher Sci., Schwerte, Germany). All chemicals and reagents were of the highest degree of purity available. *Escherichia coli* strains DH10B and Rosetta2 (DE3) pLysS were used for cloning and expression studies, respectively. In general, the strains were grown aerobically under constant shaking conditions at 37 °C on lysogeny broth (LB) containing 10 g/L of NaCl and the antibiotics ampicillin and chloramphenicol with final concentrations of 100 µg/mL and 12.5 µg/mL, respectively. All information on the plasmids, expression vectors, and primer sequences used in this study can be found on Tables A1–A3.

### 2.2. Cloning and Expression

The *dyp* genes (*dypA*—RHA1\_ro05773 and *dypB*—RHA1\_ro02407) from *Rhodococcus jostii* RHA1 (CP000431.1) were compared to the sequences (*dypA*—R1CP\_10130 and *dypB*—R1CP\_29905) from *R. opacus* 1CP (CP009111.1). The genes *dypA* and *dypB* were amplified from genomic DNA of *R. opacus* 1CP using the primer pairs for *dypA* (DyPA\_1CP\_fw and DyPB\_1CP\_rev) and *dypB* (DyPB\_1CP\_fw and DyPB\_1CP\_rev) (Appendix A). The PCR products were obtained from agarose gel electrophoresis, blunt-end ligated into the

dephosphorylated HincII (for *dypA*) and SfoI (for *dypB*) restriction site of pUC19 and then propagated into *E. coli* DH10B. Plasmids were isolated from white colonies and subjected to DNA sequencing (data not shown).

Confirmed *dypA* and *dypB* genes in pUC19 were cleaved at the *NdeI* and *NotI* restriction site and ligated into the pET16bP vector. Correct clones were selected by colony PCR and expression plasmids were sent for DNA sequencing using T7- and T7 term- primers. Plasmids with the confirmed *dyp* genes constructs were then transformed to *E. coli* Rosetta (DE3) pLysS.

For gene expression, precultures of the expression clones were made by inoculating the *E. coli* harboring *dypA* and *dypB* in an LB medium and then subsequently placed the cultures at 37 °C at 150 rpm overnight. Precultures were then transferred into a 500 mL fresh LB medium containing the antibiotics, ampicillin and chloramphenicol, with the aforementioned concentration and 16 µM hemin. Expression cultures were cultivated at 37 °C at 150 rpm. Once the cultures reach an OD<sub>600</sub> of about 0.5, the temperature was decreased to 20 °C and subsequently induced with 0.1 mM IPTG (isopropyl-β-D-1-thiogalactopyranoside). Cells were harvested at 4 °C by centrifugation (5000 rpm, 20 min) and cell pellets were frozen at −20 °C.

### 2.3. Enzyme Purification, Quantification, and Verification

Cell pellets were thawed and resuspended in 4-fold volume of TED buffer (25 mM Tris-HCl, 2 mM EDTA, 2 mM DTT, pH 8.0) plus the lysozyme solution (25 mM Tris-HCl, 1% lysozyme, pH 8.0) and incubated for 30 min on ice before disruption via ultrasonication. The soluble proteins were separated from the cell debris by centrifugation at 4 °C (18,500 rpm, 40 min).

His-tagged DyPs were purified on a Ni-sepharose column (45 mL Ni<sup>2+</sup> loaded Chelating Sepharose Fast Flow (Amersham Bioscience), using ECONO system (BIO-RAD) laboratories equipped with a UV monitor and tempered at 4 °C. DypA-containing crude extracts were spiked with 500 mM NaCl prior to loading. The column was pre-equilibrated with a filtered and degassed mixture of Buffer A (DypA: 25 mM Tris-HCl, 500 mM NaCl, pH 8.0; DypB: 25 mM Tris-HCl, pH 8.0) and Buffer B (Buffer A plus 500 mM (DypA) or 400 mM (DypB) imidazole) which was 90%:10% for Dyp A and 95%:5% for DypB, respectively. Proteins were eluted by a linear gradient of increasing imidazole concentration from 10% to 100% Buffer B over 12 column volumes. Eight ml fractions were collected and assayed for peroxidase activity, protein content, and purity via SDS-PAGE. Pure and most active fractions were pooled, dialyzed against 200-fold volume 10mM Tris-HCl buffer (pH 8.0) and stored in aliquots at −20 °C.

Bradford assay was used to determine protein concentration, using bovine serum albumin (BSA) as a standard. Meanwhile, sodium dodecyl sulfate polyacrylamide gel (SDS-PAGE) was used to verify the purity of the proteins and to determine the sizes.

### 2.4. Enzyme Characterization

Two assays were used to characterize DypA and DypB. First, peroxidase activity was determined spectrophotometrically using the 2,2'-azino-bis [3-ethylbenzthiazoline-6-sulphonic acid] (ABTS)-assay. Standard ABTS assay contained 1 mM ABTS, 0.1 M KPi buffer at pH 5.0, 0.25 mM H<sub>2</sub>O<sub>2</sub> and the corresponding enzyme. After mixing, the increase in extinction at 420 nm was recorded for 1 min at room temperature. ABTS assay was further optimized to determine the best conditions for the DyPs from *Rhodococcus opacus* 1CP. The pH profile was determined with the standard ABTS assay using Britton-Robinson buffer (25 mM KH<sub>2</sub>PO<sub>4</sub>, 25 mM H<sub>3</sub>BO<sub>3</sub>, 25 mM trisodium citrate . . . 2 H<sub>2</sub>O, 25 mM HCl, pH 2–6 with NaOH). Moreover, the influence of the buffer composition on ABTS conversion was investigated by testing different buffers such as 25 mM citrate buffer, 25 mM citric acid phosphate buffer (25 mM citric acid, 50 mM Na<sub>2</sub>HPO<sub>4</sub>), 25 mM sodium acetate buffer (25 mM sodium acetate, 25 mM acetic acid), and 25 mM KPi.

Meanwhile, dye-decolorizing peroxidase activity was determined spectrophotometrically using the Reactive Blue 5 (RB5)-assay [42]. Typically, 1 mL RB5-assay contained 500  $\mu$ L 288  $\mu$ M RB5 solution, (480-x)  $\mu$ L 25 mM citrate buffer (pH 3.6), 20  $\mu$ L 0.03% H<sub>2</sub>O<sub>2</sub> and an appropriate amount of enzyme (2.5 nM DypA and 22.6 nM DypB). After mixing, the decrease in extinction at 600 nm was detected immediately and run for 1 min at 20 °C for DypA and 30 °C for DypB.

The temperature optimum was determined for both the optimized ABTS and RB5 assay for each enzyme varying the temperature from 4–60 °C. The H<sub>2</sub>O<sub>2</sub> tolerance in the presence of ABTS was tested using the optimized ABTS assay. The H<sub>2</sub>O<sub>2</sub> concentration was varied from 0.02–200 mM.

Control reactions were performed without enzyme, H<sub>2</sub>O<sub>2</sub> or both. Conversion of substrate was only observed when both enzyme and H<sub>2</sub>O<sub>2</sub> were present. For reference, 1 U is defined as the conversion of 1  $\mu$ mol ABTS or 1  $\mu$ mol RB5 within 1 min. Measurements were carried out at least in triplicates.

### 2.5. Dye-Decolorization Capability

Additional dyes were utilized to check if the DyPs can decolorize other dyes. The concentration of each dye was adjusted so that the initial absorbance of each was around 1 in 25 mM citrate buffer (pH 3.6). The respective final concentration in a 1 mL assay was as follows: Reactive Blue 5 (137  $\mu$ M,  $\epsilon_{600-20^\circ\text{C}} = 7.1 \text{ mM}^{-1} \text{ cm}^{-1} / \epsilon_{600-30^\circ\text{C}} = 7.3 \text{ mM}^{-1} \text{ cm}^{-1}$ ), Reactive Blue 19 (177  $\mu$ M,  $\epsilon_{595-20^\circ\text{C}} = 5.7 \text{ mM}^{-1} \text{ cm}^{-1} / \epsilon_{595-30^\circ\text{C}} = 5.9 \text{ mM}^{-1} \text{ cm}^{-1}$ ), Reactive Black 5 (56  $\mu$ M,  $\epsilon_{597-20^\circ\text{C}} = 19.2 \text{ mM}^{-1} \text{ cm}^{-1} / \epsilon_{597-30^\circ\text{C}} = 19.3 \text{ mM}^{-1} \text{ cm}^{-1}$ ), Reactive Red 23 (88  $\mu$ M,  $\epsilon_{520-20^\circ\text{C}/30^\circ\text{C}} = 11.8 \text{ mM}^{-1} \text{ cm}^{-1}$ ), Reactive Orange 16 (65  $\mu$ M,  $\epsilon_{495-20^\circ\text{C}/30^\circ\text{C}} = 14.8 \text{ mM}^{-1} \text{ cm}^{-1}$ ), Reactive Yellow 37 (69  $\mu$ M,  $\epsilon_{400-20^\circ\text{C}} = 13.3 \text{ mM}^{-1} \text{ cm}^{-1} / \epsilon_{400-30^\circ\text{C}} = 13.4 \text{ mM}^{-1} \text{ cm}^{-1}$ ), Poly R-478 (0.4  $\mu$ M,  $\epsilon_{520-20^\circ\text{C}} = 2572.5 \text{ mM}^{-1} \text{ cm}^{-1} / \epsilon_{520-30^\circ\text{C}} = 2559.4 \text{ mM}^{-1} \text{ cm}^{-1}$ ). The structures of the dyes used in this study can be seen on Figure 1. Control reactions were included as described earlier.

The extinction coefficient for each dye was determined in triplicates from a 1 mg mL<sup>-1</sup> stock solution of the dye in 25 mM citrate buffer (pH 3.6) at 20 °C and 30 °C using the LAMBERT-BEER law and taking the dilution factor of the dye in buffer into account.  $\lambda_{\text{max}}$  was ascertained for each dye performing a wave scan from 300 to 800 nm.

### 2.6. Sequence Analysis

A BLASTp search [47] of DypA and DypB sequence from *R. opacus* 1CP was performed against the NCBI database. Sequence-based alignment of Dyps and other peroxidases (out-group) was done using ClustalW [48]. The maximum likelihood tree was generated from 1000 bootstraps using Mega X [49]. NCBI accession numbers used are listed on Table A4.

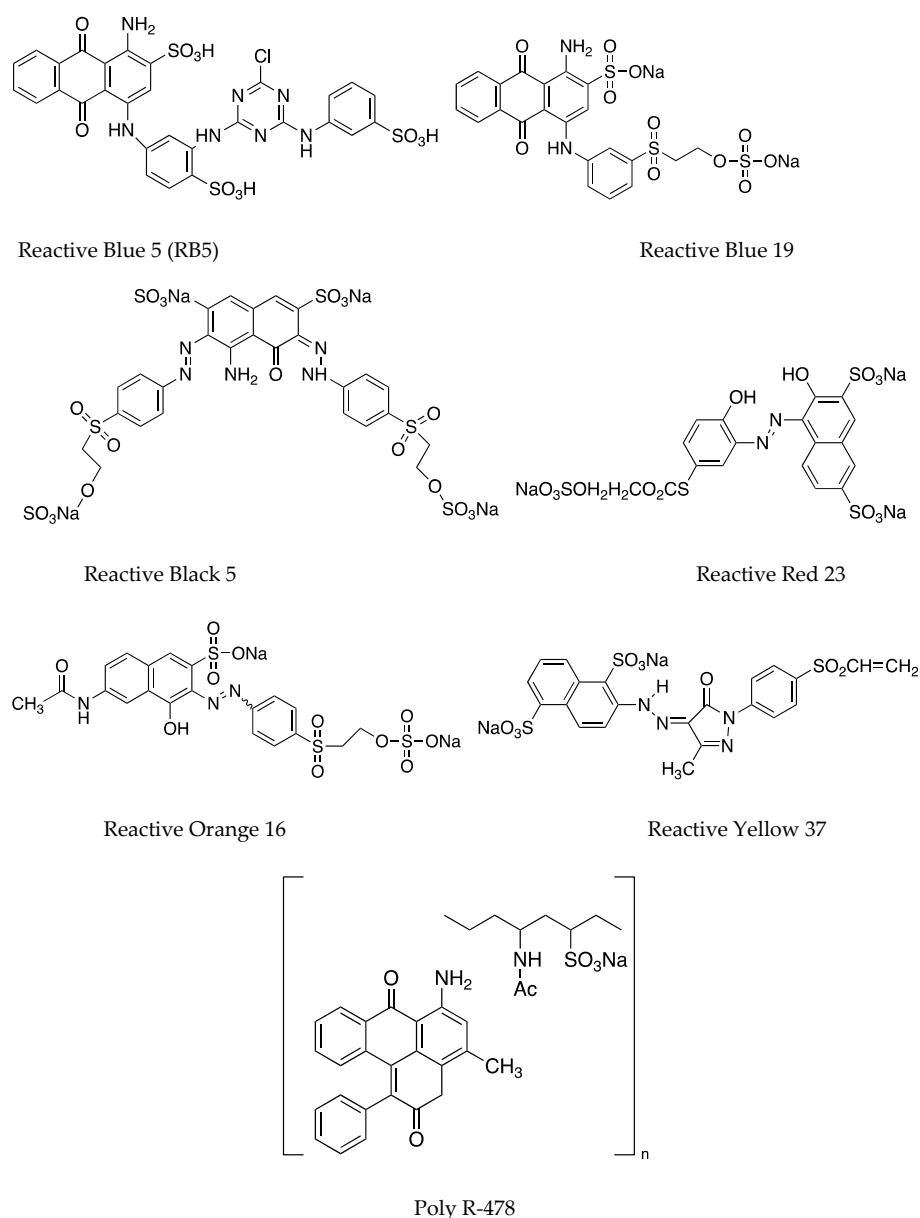


**Figure 1.** Structures of the dyes used in the study. Reactive Blue 5 (RB5) and Reactive Blue 19 represent the anthraquinone dyes. Reactive Black 5, Reactive Red 23, Reactive Orange 16, and Reactive Yellow 37 represent the azo dyes. Poly R-478 represents an anthraquinone-based polymeric dye.

### 3. Results

#### 3.1. Identification of Dyp Genes

The *dyp* genes from *Rhodococcus opacus* 1CP were compared to the DypA and DypB from *Rhodococcus jostii* RHA1 via a BLAST search. Results showed (data not shown) the DypA of *R. opacus* 1CP is 98% similar to that of *R. jostii* DypA and shared only 33% similarity to the Dyp enzyme of *Geobacillus geotrichum*. Meanwhile, DypB of *R. opacus* 1CP have 97% similarity to the DypB of *R. jostii* RHA1 and only 29% to Dyp of *G. geotrichum*.

Dye-decolorizing peroxidases are often classified into four distinct classes based on their homologies [3]. Class A, B, and C generally include Dyps of bacteria belonging to the phyla Proteobacteria, Actinobacteria, Firmicutes, and Bacteroides, while Class D includes fungal Dyps. Thereby, Class A and B form a cluster distinguishable from Class C and D indicating that they share more sequence similarities than to the other two groups. As expected, DypA and DypB from *R. opacus* 1CP are assigned to Class A and B, respectively,

and are the closest related to Dyps of other rhodococci like *R. jostii* RHA1, *R. opacus* PD630 or *R. opacus* B4 (Figure A1).

### 3.2. Biochemical Properties of DyPA and DyPB

pET16bp\_dypA and pET16bp\_dypB harboring the respective Dyp-genes were used for expression and allowed the production of recombinant proteins after induction with IPTG and upon addition of hemin. Soluble fractions of cell disruption were strongly reddish colored indicating the presence of heme-containing enzymes. Dyps were isolated on Ni-sepharose columns checking presence and purity via SDS-PAGE (Figures A2 and A3). The theoretical molecular size of 48.48 kDa (DypA) and 39.81 kDa (DypB) corresponded to the observed single band at around 50 kDa and 40 kDa, respectively.

Various parameters were checked to determine the optimal conditions for these enzymes to operate on. First, the thermal stability of DyPs were determined by incubating the enzymes up to 60 °C (Figure 2). DypA showed already a decrease of 15% in its activity at 25 °C after about 2 h of incubation while more than 20% decrease after 1 h at 30 °C. The subsequent loss of activity at 30 °C was further observed after 2 h. At 40 °C, DypA exhibited only 15% activity on the first reading and did not show further activity after 10 min. In contrast, DypB showed more heat resistance by retaining its activities even after 5 h on 30 °C. Though a decrease in activity can already be observed for DypB after 30 min at 40 °C, it was still able to retain 90% of its activities during the first 15 min of incubation. Both enzymes did not show any activity at 50 °C and 60 °C, respectively (data not shown).

Britton-Robinson buffer was used since it offers a wide range of pH to be tested. As seen on Figure 3, both Dyps from *Rhodococcus opacus* 1CP operated better on acidic pH. DypA performed best with pH 4.3 and showed a significant reduction with pH 6 (Figure 3). Meanwhile, DypB performed relatively well with a wider range of pH around pH 4–6, showing close values in its specific activity.

Different buffers were checked to determine the most suitable buffer for DypA and DypB assays. Since the best pHs for DypA and DypB were pH 4.3 and pH 5, respectively, the buffers tested were prepared with the same optimal pH relative to Britton-Robinson buffer. At pH 4.3, DypA performed twice as better on citrate buffer and citrate phosphate buffer compared to Britton-Robinson (Figure 4A). With citrate buffer, a 50% increase was observed in its activity. Sodium acetate buffer, on the other hand, showed the same activity to Britton-Robinson buffer.

DypB was also tested on the same buffers used with DypA. However, all of the buffers tested for DypA were inhibitory to the activity of DypB. Potassium phosphate buffer was checked and DypB showed an increase on its activity (Figure 4B).

Tolerance to H<sub>2</sub>O<sub>2</sub> was tested by checking different concentrations and monitored via ABTS assay. DypA obtained the highest activity with about 4 mM H<sub>2</sub>O<sub>2</sub> and sustained relatively high activity until 10 mM of H<sub>2</sub>O<sub>2</sub> (Figure 5). Meanwhile, the optimum concentration for DypB was about 3 mM H<sub>2</sub>O<sub>2</sub> then showed subsequent loss of activity. Interestingly, both Dyps still exhibited some activity at 195 mM of H<sub>2</sub>O<sub>2</sub> (Table A5).

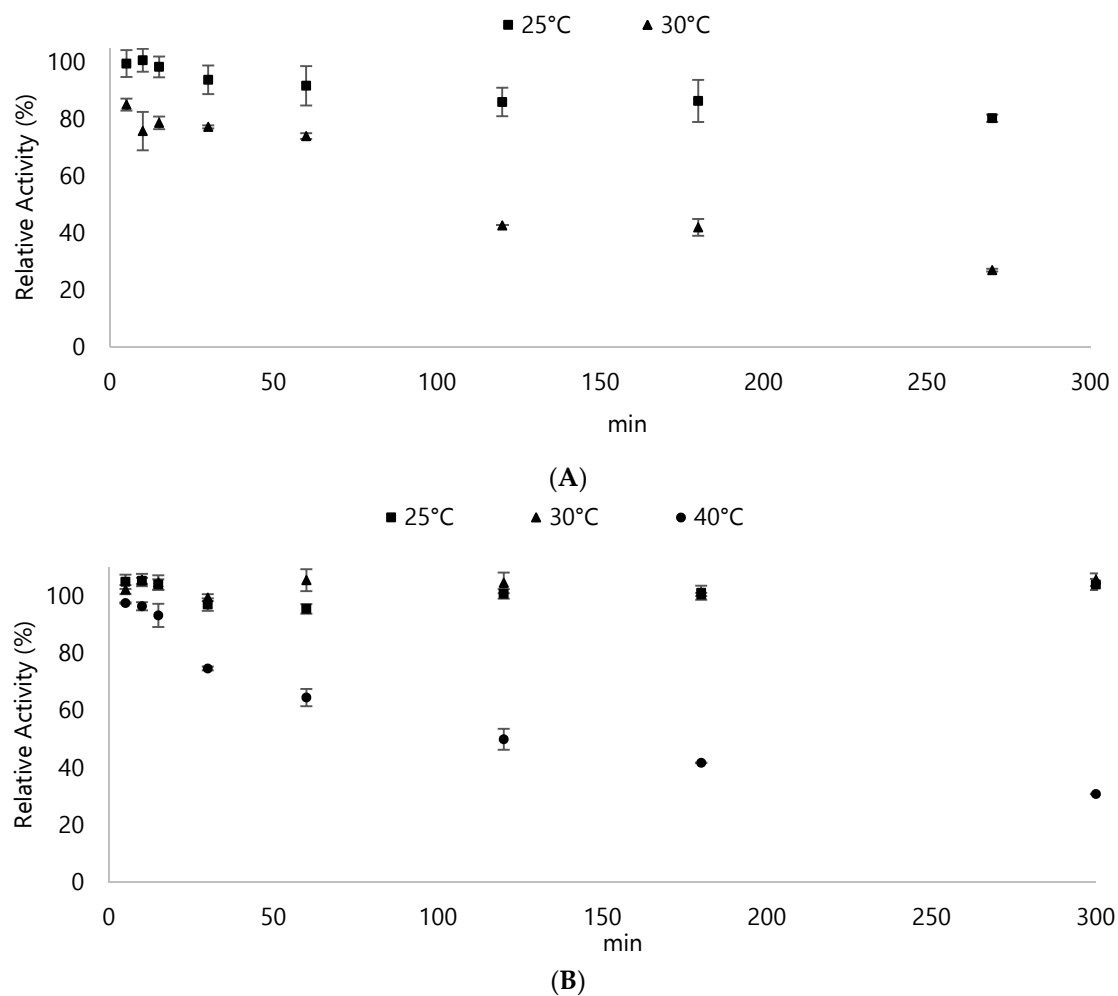


**Figure 2.** Thermal stability of (A) DypA and (B) DypB. The enzymes were incubated at different temperatures and subjected to standard ABTS assay to determine changes in the activity. DypA exhibited about 13 U/mg while DypB showed about 12 U/mg. These values represent the 100% so as to compare the relative activity of the enzyme after subsequent incubation to different temperatures. Results for higher temperatures were not shown because the enzyme was rendered inactive immediately. Assay was done in 100 mM potassium phosphate buffer (pH 5), ABTS solution, and 0.2 mM H<sub>2</sub>O<sub>2</sub>.

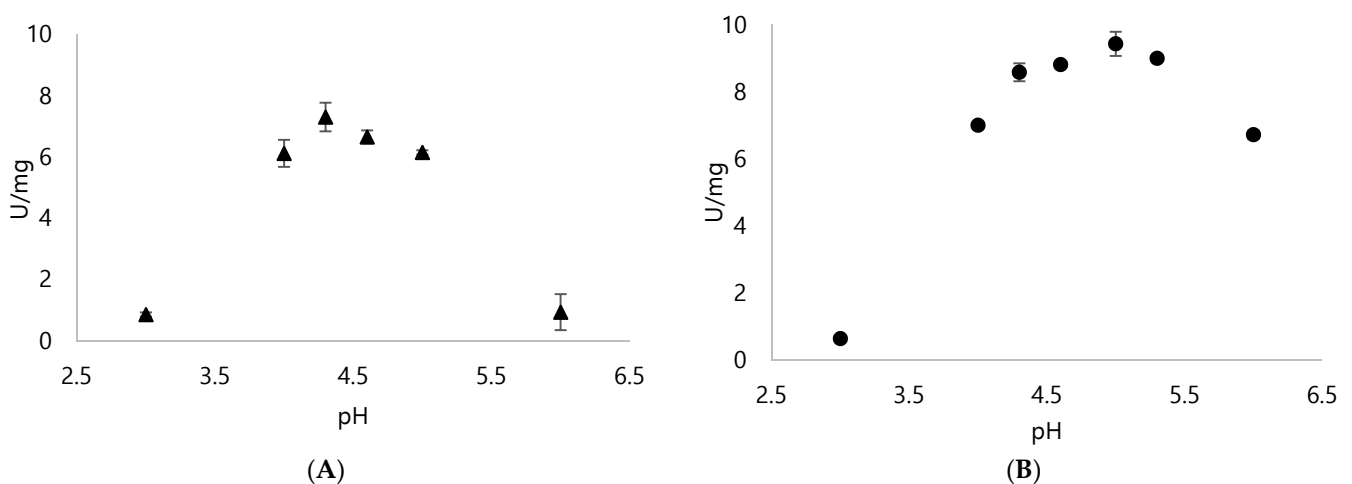


**Figure 3.** Specific activity of (A) DypA and (B) DypB with 1 mM ABTS as the substrate and 0.25 mM H<sub>2</sub>O<sub>2</sub> using Britton-Robinson buffer with pH ranges from pH 2 to 6 to check the optimal pH for each enzyme.

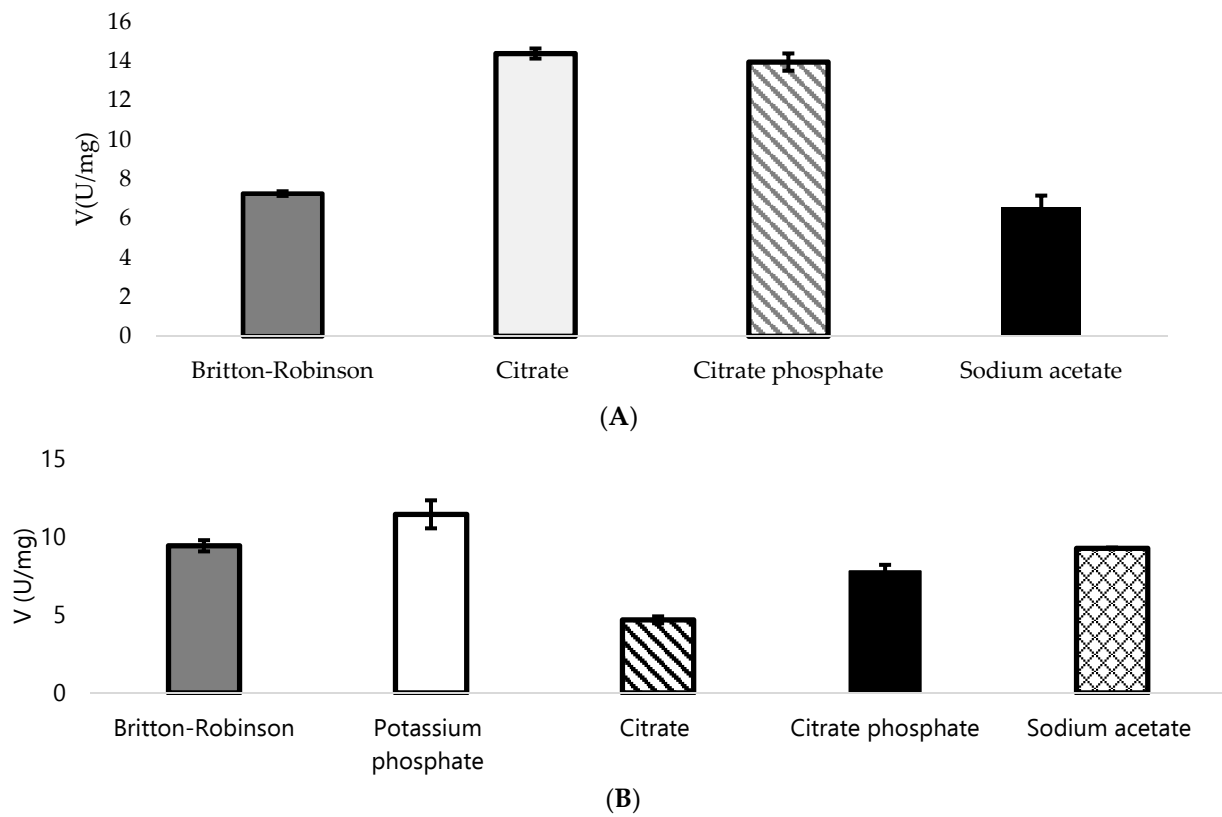


**Figure 4.** Specific activity of (A) DypA at pH 4.3 and (B) DypB at pH 5.0. Both enzymes were tested with different buffers using Britton-Robinson buffer as a standard for comparison with respect to activity. Potassium phosphate buffer was used only for DypB since most of the buffers tested showed a decrease in activity when tested to citrate, citrate phosphate, and sodium acetate buffers.

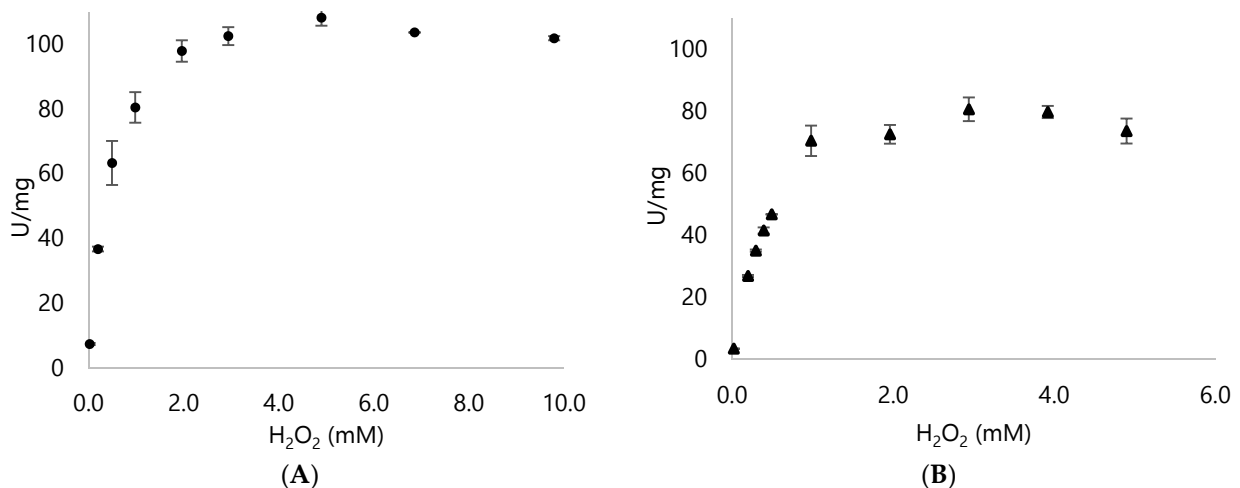


**Figure 5.** H<sub>2</sub>O<sub>2</sub> profile of the Dyps using the optimal pH and buffer for both Dyps. (A) DypA activity in citrate buffer, pH 4.3 (B) DypB activity in phosphate buffer, pH 5.0. Different H<sub>2</sub>O<sub>2</sub> concentrations were used and monitored until a decrease in activity can be seen (Table A5).

### 3.3. Activities of DyPA and DypB with RB5 as a Substrate

Aside from ABTS, Reactive Blue 5 (RB5) is also used as a standard substrate for dye-decolorizing peroxidases. The optimal reaction conditions differentiate considerably when using RB5 as a representative substrate for Dyps. Though potassium phosphate buffer showed the best activity for DypB during the ABTS assay, it showed a more significant

reduction for RB5 (data not shown). Hence, for RB5, citrate buffer was used for all assays. Both Dyps showed the best activity at pH 3.6 (Figure 6).

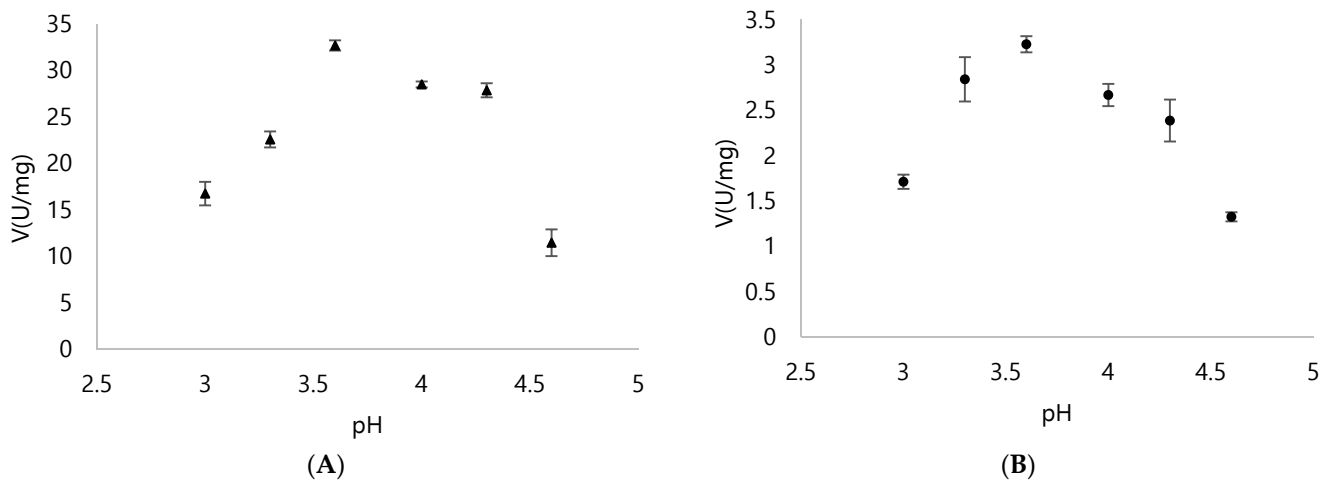


**Figure 6.** Specific activity of (A) DypA and (B) DypB with 144  $\mu$ M RB5 as the substrate using 25 mM citrate buffer to check the optimal pH for each enzyme.

Thermal stability for RB5 assay was also determined. For DypA, most reactions done at room temperature for the RB5 were relatively stable (Figure 6). In contrast to DypB, only at 30  $^{\circ}$ C that it showed a fairly stable reaction for RB5 and showed a 20% decrease in activity for other temperatures (Figure 7). This showed a stark contrast to the behavior of the Dyps since DypA exhibited more stability with RB5 than the ABTS assay while DypB had an opposite trend.

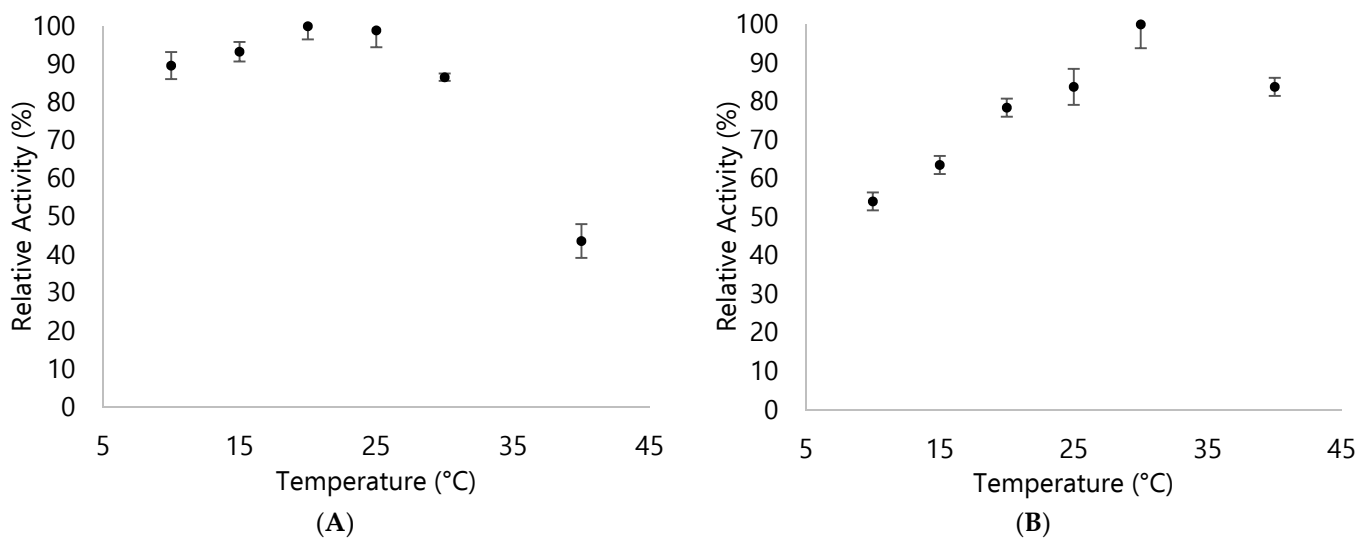


**Figure 7.** Relative activity of (A) DypA and (B) DypB with 144  $\mu$ M RB5 assay in 25 mM citrate buffer (pH 3.6) at different temperatures.

### 3.4. Kinetic Parameters for DypA and DypB

Using Reactive Blue 5 to differentiate properties between DypA and DypB of *Rhodococcus opacus* 1CP, it was shown that DypA showed better preference for the anthraquinone representative (Figures 8 and 9; Table 1).

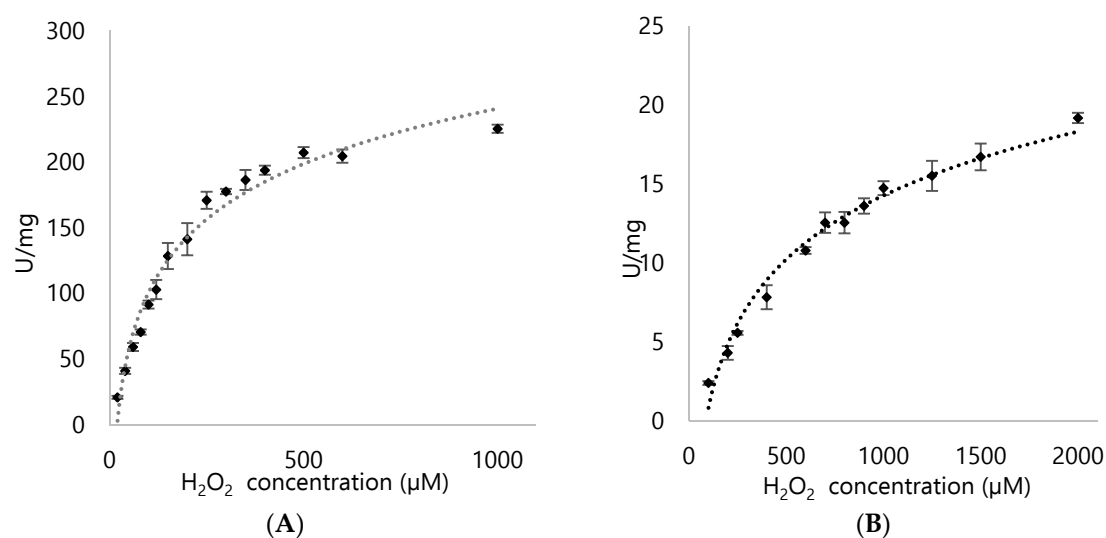


**Figure 8.** Michaelis-Menten kinetics of (A) DypA and (B) DypB with varying concentrations of H<sub>2</sub>O<sub>2</sub> (20 μM to 1000 μM) in Reactive Blue 5 assay.

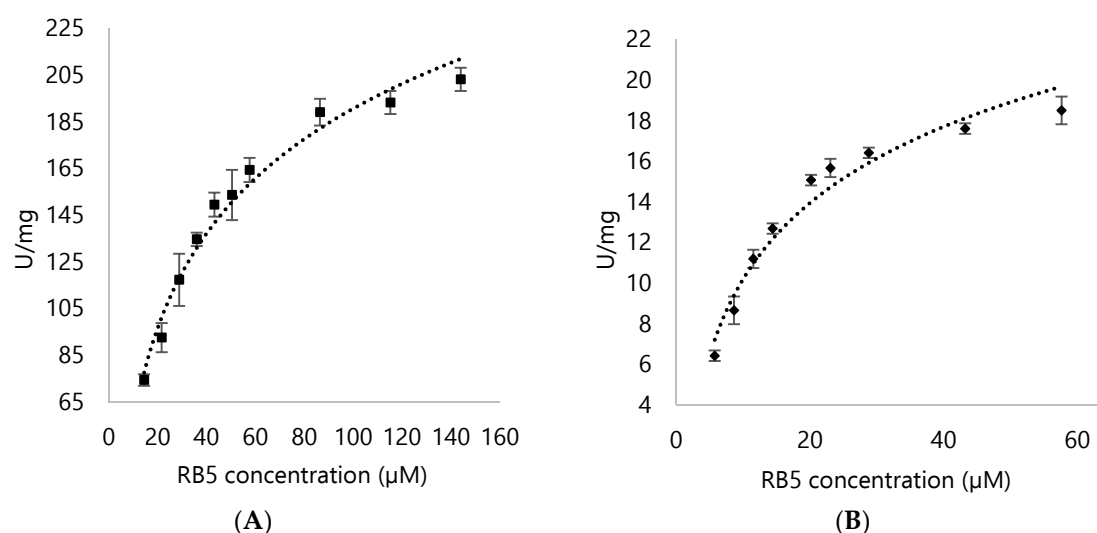


**Figure 9.** Michaelis-Menten kinetics of (A) DypA and (B) DypB with varying concentrations of Reactive Blue 5 (15 μM to 144 μM for DypA; 5 μM to 57 μM for DypB) in Reactive Blue 5 assay.

**Table 1.** Steady-state kinetic parameters of DypA and DypB towards H<sub>2</sub>O<sub>2</sub> and Reactive Blue 5. Calculation of these parameters were based from the Michaelis-Menten fit from Figures 8 and 9.

Enzyme	Substrate	K <sub>m</sub> (μM)	V <sub>max</sub> (U/mg)	K <sub>cat</sub> (s <sup>-1</sup> )	K <sub>cat</sub> /K <sub>m</sub> (μM/s <sup>-1</sup> )
DypA	H <sub>2</sub> O <sub>2</sub>	196.89 ± 16.95	282.39 ± 9.52	228.17 ± 7.69	1.16 ± 0.45
	RB5	33.34 ± 2.37	254.6 ± 6.69	205.72 ± 5.41	6.17 ± 2.28
DypB	H <sub>2</sub> O <sub>2</sub>	1011.8 ± 78.15	28.74 ± 1.11	19.07 ± 0.89	0.018 ± 0.011
	RB5	12.78 ± 1.15	23.21 ± 0.96	15.47 ± 0.78	1.21 ± 0.68

### 3.5. DypA and DypB Activities against Different Dyes

Seven dyes were tested to check the dye-decolorizing capability of Dyps. The dyes were comprised of two anthraquinone dyes (Reactive Blue 5 and Reactive Blue 19), diazo dye (Reactive Black 5), copper complex azo dye (Reactive Red 23), single azo dyes (Reactive Orange 16 and Reactive Yellow 37), and the polyanthraquinone dye with poly(vinylamine) sulfonate backbone (Poly R-478).

DypA showed strong preferences for the two anthraquinone representatives as it exhibited about  $114 \pm 2.94$  U/mg and  $5.91 \pm 0.6$  U/mg for Reactive Blue 5 and Reactive Blue 19, respectively. Reactive Black 5 and Reactive Red 23 were also moderately accepted but not as efficient compared to the two anthraquinone dyes. DypB, on the other hand, only showed activity against the two anthraquinone dyes. Interestingly, both dyes did not have any activity on single azo dye structures used in this study. Poly R-478, an anthraquinone-based polymeric dye, was somewhat acted on by DypA. However, it only showed a low activity of  $1.15 \pm 0.4$  mU/mg at  $0.4 \mu\text{M}$  concentration of Poly R-478.

Overall, DypA was a better dye converter than DypB as it acted on about 4 dyes out of the 7 that were tested. However, the substrate scope of the DypA and DypB from *Rhodococcus opacus* 1CP was still not up to par compared to known dye-decolorizing peroxidases.

#### 4. Discussion

This paper establishes that *Rhodococcus opacus* 1CP has similar dye-decolorizing peroxidases (DypA and DypB) described for *Rhodococcus jostii* RHA1 (Figure A1).

Dye-decolorizing peroxidases are heme-containing enzymes [50]. However, the heterologous expression in *E. coli* limits the production of soluble, active heme-containing enzymes since it doesn't incorporate heme efficiently. Incomplete or inefficient heme incorporation into recombinant proteins have been frequently described [51–53] especially in the induction of recombinant protein expression systems from highly active vectors such as *E. coli* expression hosts with T7 promoters. This usually leads to high protein production of enzyme without the heme cofactor. Various techniques have been employed such as the co-expression of  $\delta$ -aminolevulinic acid to enhance internal heme production and the reconstitution of apoenzyme with hemin chloride [30,54–56]. In this study, the supplementation of hemin in growth medium showed good results [57]. A total of 3.72 mg of DypA were purified from 10.8 g of *E. coli* cells (wet weight) and 16.56 mg of DypB were purified from 7.8 g of *E. coli* cells (wet weight).

Both DyPs from *R. opacus* 1CP contain highly conserved residues that are essential for its enzymatic activity: GxxDG with the conserved Asp, distal Arg, and proximal His. Several studies [58–60] have been done to show that these motifs play a major role on the stability, heme-binding, and biocatalysis of dye peroxidases. The preference of DyP-type peroxidases to utilize Asp as an acid-base catalyst explains the high activity of these enzymes at low pH since the pKa of Asp is at 3.9 [61,62]. Meanwhile, the thermostability of DypA and DypB vary from each other. DypB showed more stability at 25 and 30 °C while DypA already exhibited decrease in activity even at room temperature. Though DypB showed subsequent decrease in activity at 40 °C after 15 min, DypA was already rendered inactive at this temperature.

Suicide inactivation via excessive  $\text{H}_2\text{O}_2$  exposure is one of the biggest hurdles when working with peroxidases. The formation of Compound III leads to cofactor destruction, release of heme iron or oxidation of amino acid side chains [63–65]. For this reason, the standard ABTS assay use only up to 0.2 mM  $\text{H}_2\text{O}_2$ . However, the Dyp enzymes of *R. opacus* 1CP exhibited enzymatic activities at higher concentrations of  $\text{H}_2\text{O}_2$ . The activity of DypA was retained from 3.9 mM up to about 10 mM before showing decrease in activity while the activity of DypB retained its activity from 2.9 mM up to 5 mM of  $\text{H}_2\text{O}_2$  (Table A5) without any detrimental effects. It is still unclear why both enzymes are not inactivated by high concentrations of  $\text{H}_2\text{O}_2$ . Most DyPs operate only between 0.1 mM and 0.4 mM  $\text{H}_2\text{O}_2$  [22,66]. It has not been investigated yet whether DypA and DypB function as catalase-peroxidase. Most enzymes which can tolerate high concentrations of  $\text{H}_2\text{O}_2$  belong to other types of peroxidases. For example, manganese peroxidases (MnP) from *Lenzites betulinus* retained more than 60% of the initial activity after exposure to 10 mM  $\text{H}_2\text{O}_2$  for 5 min at 37 °C [67].

The results obtained from the kinetic parameters show that DypA was the more efficient catalyst for RB5. Interestingly, both enzymes showed very high  $K_m$  towards  $\text{H}_2\text{O}_2$ . A result that is very unusual for peroxidases, but this could be an explanation why it can tolerate high concentrations of  $\text{H}_2\text{O}_2$ . Despite the lower  $K_m$  of DypB for RB5, DypA still

exhibited better  $K_{cat}$  and higher  $K_{cat}/K_m$ . The poor performance of DypB for RB5 can be because that DypB might play a bigger role on lignin degradation than dye degradation. A study [30] showed that the deletion of *dypB* in *R. jostii* RHA1 led to impaired activities for lignin breakdown and the deletion of *dypA* did not show the same effect.

As the name suggests, dye-decolorizing peroxidases were believed to play a role in decolorizing a wide array of dyes such as azo dyes, heterocyclic dyes, and anthraquinone dyes [26,68]. These enzymes are known to attack the anthraquinone skeleton. In contrast to other DyPs, DypA from *R. opacus* 1CP did not show a huge substrate scope. Although it exhibited the best activity against RB5 and Reactive Blue 19, the azo dyes, Reactive Black 5 and Reactive Red 23, were only accepted up to some extent. As for DypB, it only moderately accepted RB5 and Reactive Blue 19 but not comparable to the activity of DypA. This strongly suggests that DypB of *R. opacus* 1CP has only a minimal role for dye decolorization.

## 5. Conclusions

This work offers insights to the enzymatic properties of the recombinant DypA and DypB from *Rhodococcus opacus* 1CP. Moreover, the addition of hemin to expression cultures led to enhanced heme incorporation when using *E. coli* as expression hosts. Therefore, it generated high amount of functional DypA and DypB. Although both enzymes have shown activities against ABTS and RB5, DypA performed better than DypB. Both enzymes also showed tolerance to high  $H_2O_2$  concentrations but poorly degraded dyes, suggesting that dyes are not their physiological substrate. It is also noteworthy to investigate if DypB does play a role on lignin degradation. Moreover, a study [69] showed that the dye-decolorizing peroxidase PfDyP B2 from *Pseudomonas fluorescences* Pf0-1 can insert carbene into an N-H bond. Investigation of these non-natural reactions can be a nice addition to the enzymatic reactions that these dye-decolorizing peroxidases can do.

**Author Contributions:** Conceptualization, D.T. and K.-H.v.P.; methodology, C.C. and A.M.; validation, C.C., A.C.R.N. and A.M.; formal analysis, C.C., A.C.R.N. and D.T.; investigation, C.C.; resources, K.-H.v.P.; data curation, C.C., Á.G.B. and A.C.R.N.; writing—original draft preparation, C.C. and A.C.R.N.; writing—review and editing, A.C.R.N., D.T. and K.-H.v.P.; supervision, A.M., D.T. and K.-H.v.P.; project administration, D.T.; funding acquisition, D.T. and K.-H.v.P. All authors have read and agreed to the published version of the manuscript.

**Funding:** We acknowledge funding of this project by the European Social Fund, and the Saxonian Government (GETGEOWEB 100101363).

**Institutional Review Board Statement:** Not applicable.

**Informed Consent Statement:** Not applicable.

**Data Availability Statement:** Not applicable.

**Acknowledgments:** We like to thank Michael Schlömann (TU Bergakademie Freiberg) for the support during the experimental phase. Further, we thank the DFG Research Training Group GRK 2341 “Microbial Substrate Conversion (MiCon)” for support and training of our graduate students.

**Conflicts of Interest:** The authors declare no conflict of interest.

## Appendix A

The appendix comprises of the information regarding the strains, primers, and plasmids used in the study. It also contains the information on the different classes of DyPs and SDS-PAGE information for DypA and DypB.

**Table A1.** Donor, intermediate and expression hosts.

Strain	Term	Attributes	Supplier/Reference
<i>R. opacus</i> 1CP	-	donator; Gram-positive actinobacterium	Environmental Microbiology Group, TU Freiberg [70]
<i>E. coli</i> DH10B	-	intermediate host; blue-white-selection	Invitrogen, Karlsruhe, Germany Biological Institute, TU Dresden
<i>E. coli</i> Rosetta2 (DE3) pLysS	R2	expression host; cam <sup>R</sup> ; derivative of <i>E. coli</i> BL21 (DE3) pLysS, additional supply of tRNAs for 7 rare codons (AGA, AGG, AUA, CUA, GGA, CCC, CGG)	MERCK Millipore, Darmstadt, Germany Strain Collection, Institute for Chemistry, TU Dresden
<i>E. coli</i> Rosetta2 (DE3) pLysS_pET16bp	R2pet	expression host; derivative of <i>E. coli</i> Rosetta2 (DE3) pLysS, additionally harbors pET16bp	this study
<i>E. coli</i> Rosetta2 (DE3) pLysS_pET16bp_dypA	R2A	expression host; derivative of <i>E. coli</i> Rosetta2 (DE3) pLysS, capable of producing recombinant DypA	this study
<i>E. coli</i> Rosetta2 (DE3) pLysS_pET16bp_dypB	R2B	expression host; derivative of <i>E. coli</i> Rosetta2 (DE3) pLysS, capable of producing recombinant DypA	this study

**Table A2.** Plasmids used in this study.

Plasmid	Attributes	Supplier/Reference
pUC19	cloning vector, 2686 bp, <i>bla</i> (amp <sup>R</sup> ), <i>lacZ</i> α for blue-white selection	supplied by Dr. S. Flecks (Biochemistry, TU Dresden)
pUC19_dypA	plasmid derived from pUC19 containing <i>dypA</i> (gene of interest)	this study
pUC19_dypB	plasmid derived from pUC19 containing <i>dypB</i> (gene of interest)	this study
pET16bp	expression vector derived from pET16b with expanded MCS, 5740 bp, <i>bla</i> (amp <sup>R</sup> ), T7 promoter, <i>lacI</i> repressor, allows expression of recombinant proteins with N-terminal His <sub>10</sub> -tag	supplied by Dr. D. Tischler (Environmental Microbiology Group, TU Freiberg)
pET16bp_dypA	plasmid derived from pET16bp containing <i>dypA</i> (gene of interest)	this study
pET16bp_dypB	plasmid derived from pET16bp containing <i>dypB</i> (gene of interest)	this study

Abbreviations: bp = base pair, *bla* = beta-lactamase, amp = ampicillin, R = resistance

**Table A3.** Primers used for PCR amplification and sequencing.

Primer	Sequence 5'→3'	Specification and Use
DypA_1CP_fw	CATATGATCATGACTGATCCGACCG	with NdeI restriction site, used for PCR amplification of <i>dypA</i> in order to clone it into pUC19 and pET16bp
DypA_1CP_rev	GCGGCCGCAGGCTCTACGTGAACAG	with NotI restriction site, used for PCR amplification of <i>dypA</i> in order to clone it into pUC19 and pET16bp
DypB_1CP_fw	CATATGCCAGGCCAGTCGCGAG	with NdeI restriction site, used for PCR amplification of <i>dypB</i> in order to clone it into pUC19 and pET16bp
DypB_1CP_rev	GCGGCCGCTCATTGCGATACTCT	with NotI restriction site, used for PCR amplification of <i>dypB</i> in order to clone it into pUC19 and pET16bp
M13 uni (-21)	TGTA AACGACGGCCAGT	forward sequencing primer used to verify <i>dypA</i> in pUC19
pUC19_seq_fw	CTTA ACTATGCGGCATCAGAGCAGA	forward sequencing primer used to verify <i>dypB</i> in pUC19
M13 rev (-49)	GAGCGGATAACAATTCACACAGG	reverse sequencing primer used to verify <i>dypA</i> and <i>dypB</i> in pUC19
T7	TAATACGACTCACTATAGGG	forward sequencing primer used to verify <i>dypA</i> and <i>dypB</i> in pET16bp
T7 term	CTAGTTATTGCTCAGCGGT	reverse sequencing primer used to verify <i>dypA</i> and <i>dypB</i> in pET16bp

**Table A4.** Selection of described Dyps and affiliation to domain and phyla.

Domain/Phyla	Name	Species	NCBI Accession nr.
Fungi	DyP	<i>Galactomyces geotrichum</i> Dec1	Q8WZK8
	MsP1	<i>Marasmius scorodoni</i>	B0BK71
	MsP1	<i>Marasmius scorodoni</i>	B0BK71
	MsP2	<i>Marasmius scorodoni</i>	B0BK72
	AjP1	<i>Auricularia auricula-judae</i> 11326	AFJ79723
	PoDyp	<i>Pleurotus ostreatus</i>	CAK55151
	EglDyp	<i>Exidia glandulosa</i>	AFJ79724
	MegDyp	<i>Mycena epipterygia</i>	AFJ79725
	TAP	<i>Termitomyces albuminosus</i>	Q8NKF3
	CpoP21	<i>Polyporaceae</i> sp.	P87212
	Lbi2	<i>Laccaria bicolor</i> S238N-H82	EDR12662
	Bfu	<i>Botryotinia fuckeliana</i> B05.10	EDN26366
	PplDyp	<i>Postia placenta</i> Mad-698-R	EED79944
	AfuDyp	<i>Aspergillus fumigatus</i> Af293	EAL86784
	PchDyp	<i>Penicillium chrysogenum</i> Wisconsin 54-1255	CAP99029
Bacteria/ $\alpha$ -Proteo-	PdeDyp	<i>Paracoccus denitrificans</i> PD1222	ABL69832
	RpaDyp	<i>Rhodopseudomonas palustris</i> BisB18	ABD87513
	OanDyp	<i>Ochrobactrum anthropi</i> ATCC 49188	ABS17389
Bacteria/ $\beta$ -Proteo-	CteDyp	<i>Comamonas testosteroni</i> KF-1	EED66859
	CviDyp	<i>Chromobacterium violaceum</i> ATCC 12472	AAQ59612
Bacteria/ $\gamma$ -Proteo-	YfeX	<i>Escherichia coli</i> K12	BAE76711
	YfeB	<i>Escherichia coli</i> K12	NP_415538
	TyrA	<i>Shevanella oneidensis</i>	Q8EIU4
	AcspDyp	<i>Acinetobacter</i> sp. ADP1	CAG67144
	PsspDyp	<i>Psychrobacter</i> sp. PRwf-1	ABQ94167
Bacteria/ $\delta$ -Proteo-	PpaDyp	<i>Plesiocystis pacifica</i> SIR-1	EDM76509
	MxaDyp	<i>Myxococcus xanthus</i> DK 1622	ABF90727
Bacteria/ $\epsilon$ -Proteo-	CcoDyp	<i>Campylobacter concisus</i> 13826	EAT98288
Bacteria/Actino-	DypA	<i>Rhodococcus opacus</i> PD630	ZP_18275609
	DypA	<i>Rhodococcus opacus</i> B4	YP_002783029
	DypA	<i>Rhodococcus jostii</i> RHA1	ABG97551
	DypA	<i>Rhodococcus opacus</i> 1CP	ANS26740
	DypB	<i>Rhodococcus opacus</i> PD630	ZP_18285374
	DypB	<i>Rhodococcus opacus</i> B4	YP_002779326
	DypB	<i>Rhodococcus jostii</i> RHA1	ABG94212
	DypB	<i>Rhodococcus opacus</i> 1CP	ANS30609
	TfuDyp	<i>Thermobifida fusca</i> YX	Q47KB1
	MvaDyp	<i>Mycobacterium vanbaalenii</i> PYR-1	ABM12972
	Mtu	<i>Mycobacterium tuberculosis</i> H37Rv	CAB09574
Bacteria/Bacteroidetes	BtDyp	<i>Bacteroides thetaiotaomicron</i> Vpi-5482	2GVK_A
	ChuDyp	<i>Cytophaga hutchinsonii</i> ATCC 33406	ABG59511
Bacteria/Firmicutes	BsuDyp	<i>Bacillus subtilis</i> 168	CAB15852
Bacteria/Cyano-	AnaPx	<i>Anabaena</i> sp. PCC 7120	Q8YWM0
	AnaVT	<i>Anabaena variabilis</i> ATCC 29413	Q3M5E1
	SnyDyp	<i>Cyanothece</i> sp. PCC 8801	YP_002373279
	CyspDyp	<i>Cyanothece</i> sp. PCC 7424	ACK71272
	DdiDyp	<i>Dictyostelium discoideum</i> AX4	EAL70759

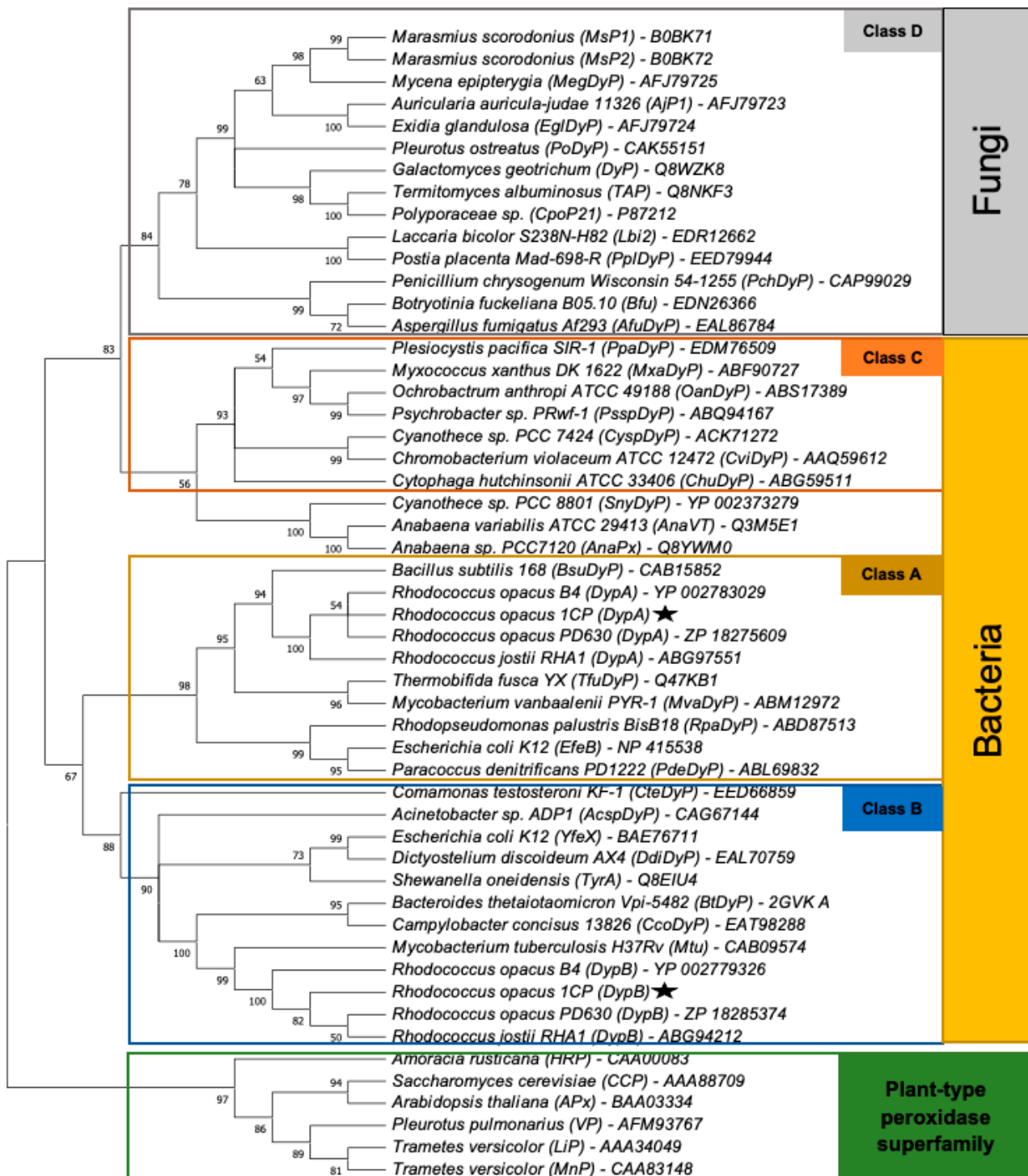


**Figure A1.** Cladogram of the dye-decolorizing peroxidase superfamily including DypA and DypB from *R. opacus* 1CP and important representatives of the plant-type peroxidase superfamily. The tree was inferred using the maximum likelihood method and JTT matrix-based model (CITE). Bootstrap values (%) were generated from 1000 replicates. This analysis involved 52 amino acid sequences.

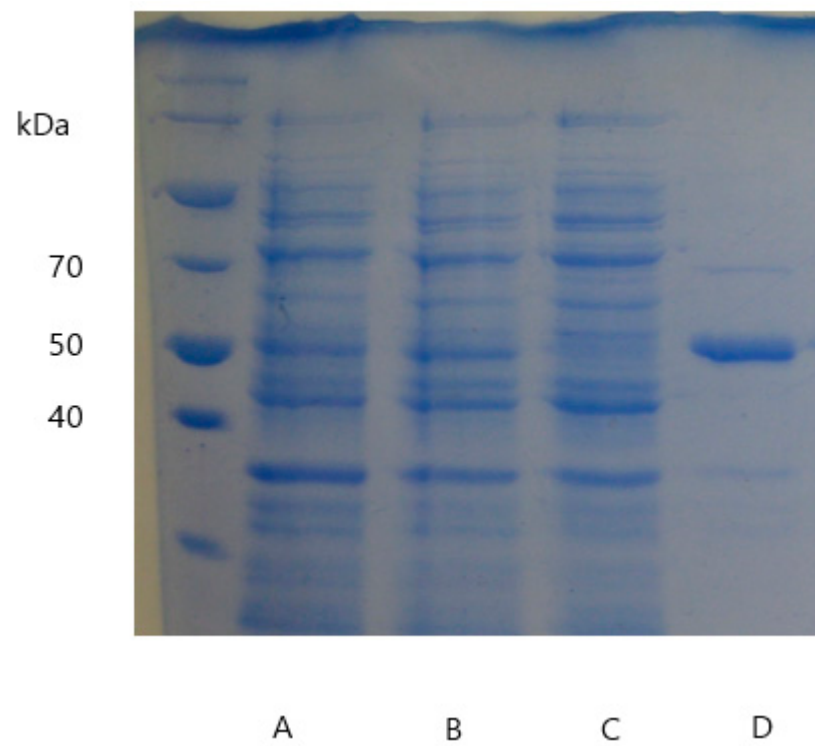


**Figure A2.** Results of SDS-PAGE illustrating the (A) crude extract, (B) crude extract after 500 mM NaCl, (C) flowthrough, (D) elution during the purification of DypA.

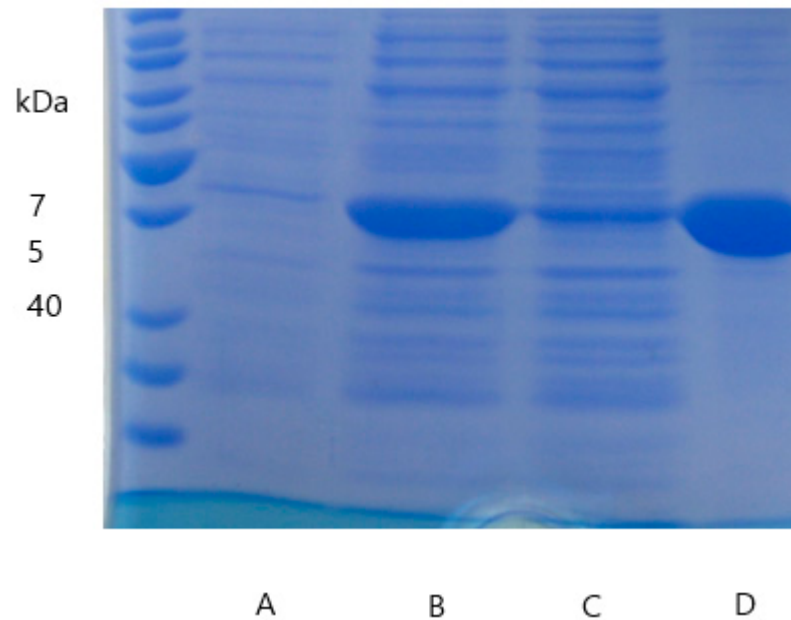


**Figure A3.** Results of SDS-PAGE illustrating the (A) negative control, (B) crude extract, (C) flowthrough, (D) elution during the purification of DypB.

**Table A5.** Specific activity of DypA and DypB at different H<sub>2</sub>O<sub>2</sub> concentrations.

H <sub>2</sub> O <sub>2</sub> conc. (mM)	DypA (U/mg)	DypB (U/mg)
0.2	36.65 ± 0.75	26.82 ± 0.34
0.5	63.24 ± 6.82	46.67 ± 0.03
1.0	80.4 ± 4.72	70.37 ± 4.91
2.0	97.84 ± 3.31	72.43 ± 3.02
2.9	102.44 ± 2.75	80.50 ± 3.82
4.9	108.15 ± 2.51	79.63 ± 1.96
9.8	101.79 ± 0.65	58.69 ± 3.96
195.8	54.03 ± 4.05	49.69 ± 1.6

## References

- Soetaert, W.; Vandamme, E.J. The scope and impact of industrial biotechnology. In *Industrial Biotechnology: Sustainable Growth and Economic Success*; Wiley-VCH Verlag GmbH & Co. KGaA: Weinheim, Germany, 2010.
- Bornscheuer, U.T.; Buchholz, K. Highlights in biocatalysis—historical landmarks and current trends. *Eng. Life Sci.* **2005**, *5*, 309–323. [[CrossRef](#)]
- Chatha, S.A.S.; Asgher, M.; Iqbal, H.M. Enzyme-based solutions for textile processing and dye contaminant biodegradation—A review. *Environ. Sci. Pollut. Res.* **2017**, *24*, 14005–14018. [[CrossRef](#)]
- Colpa, D.I.; Fraaije, M.W.; van Bloois, E. DyP-type peroxidases: A promising and versatile class of enzymes. *J. Ind. Microbiol. Biotechnol.* **2014**, *41*, 1–7. [[CrossRef](#)]
- Singh, R.; Eltis, L.D. The multihued palette of dye-decolorizing peroxidases. *Arch. Biochem. Biophys.* **2015**, *574*, 56–65. [[CrossRef](#)] [[PubMed](#)]
- Hofrichter, M.; Ullrich, R. Oxidations catalyzed by fungal peroxygenases. *Curr. Opin. Chem. Biol.* **2014**, *19*, 116–125. [[CrossRef](#)]
- Hofrichter, M.; Ullrich, R.; Pecyna, M.J.; Liers, C.; Lundell, T. New and classic families of secreted fungal heme peroxidases. *Appl. Microbiol. Biotechnol.* **2010**, *87*, 871–897. [[CrossRef](#)]
- Sugano, Y. DyP-type peroxidases comprise a novel heme peroxidase family. *Cell. Mol. Life Sci.* **2009**, *66*, 1387–1403. [[CrossRef](#)] [[PubMed](#)]
- Falade, A.O.; Mabinya, L.V.; Okoh, A.I.; Nwodo, U.U. Biochemical and molecular characterization of a novel dye-decolourizing peroxidase from *Raoultella ornithinolytica* OKOH-1. *Int. J. Biol. Macromol.* **2019**, *121*, 454–462. [[CrossRef](#)] [[PubMed](#)]
- Falade, A.O.; Nwodo, U.U.; Iweriebor, B.C.; Green, E.; Mabinya, L.V.; Okoh, A.I. Lignin peroxidase functionalities and prospective applications. *MicrobiologyOpen* **2017**, *6*, e00394. [[CrossRef](#)]
- de Gonzalo, G.; Colpa, D.I.; Habib, M.H.; Fraaije, M.W. Bacterial enzymes involved in lignin degradation. *J. Biotechnol.* **2016**, *236*, 110–119. [[CrossRef](#)] [[PubMed](#)]
- Moreno, A.D.; Ibarra, D.; Alvira, P.; Tomás-Pejó, E.; Ballesteros, M. A review of biological delignification and detoxification methods for lignocellulosic bioethanol production. *Crit. Rev. Biotechnol.* **2015**, *35*, 342–354. [[CrossRef](#)]
- Zakzeski, J.; Bruijninx, P.C.; Jongerius, A.L.; Weckhuysen, B.M. The catalytic valorization of lignin for the production of renewable chemicals. *Chem. Rev.* **2010**, *110*, 3552–3599. [[CrossRef](#)] [[PubMed](#)]
- FitzPatrick, M.; Champagne, P.; Cunningham, M.F.; Whitney, R.A. A biorefinery processing perspective: Treatment of lignocellulosic materials for the production of value-added products. *Bioresour. Technol.* **2010**, *101*, 8915–8922. [[CrossRef](#)] [[PubMed](#)]
- Lambertz, C.; Ece, S.; Fischer, R.; Commandeur, U. Progress and obstacles in the production and application of recombinant lignin-degrading peroxidases. *Bioengineered* **2016**, *7*, 145–154. [[CrossRef](#)]
- Conesa, A.; Punt, P.J.; van den Hondel, C.A. Fungal peroxidases: Molecular aspects and applications. *J. Biotechnol.* **2002**, *93*, 143–158. [[CrossRef](#)]
- Arnao, M.B.; Acosta, M.; del Rio, J.A.; Varon, R.; Garcia-Canovas, F. A kinetic study on the suicide inactivation of peroxidase by hydrogen peroxide. *Biochim. Biophys. Acta BBA-Protein Struct. Mol. Enzymol.* **1990**, *1041*, 43–47. [[CrossRef](#)]
- Lauber, C.; Schwarz, T.; Nguyen, Q.K.; Lorenz, P.; Lochnit, G.; Zorn, H. Identification, heterologous expression and characterization of a dye-decolorizing peroxidase of *Pleurotus sapidus*. *AMB Express* **2017**, *7*, 1–15. [[CrossRef](#)]
- Colpa, D.I.; Lončar, N.; Schmidt, M.; Fraaije, M.W. Creating oxidase–peroxidase fusion enzymes as a toolbox for cascade reactions. *ChemBioChem* **2017**, *18*, 2226. [[CrossRef](#)]
- Singh, R.; Grigg, J.C.; Qin, W.; Kadla, J.F.; Murphy, M.E.; Eltis, L.D. Improved manganese-oxidizing activity of DypB, a peroxidase from a lignolytic bacterium. *ACS Chem. Biol.* **2013**, *8*, 700–706. [[CrossRef](#)] [[PubMed](#)]
- Brissos, V.; Tavares, D.; Sousa, A.C.; Robalo, M.P.; Martins, L.O. Engineering a bacterial DyP-type peroxidase for enhanced oxidation of lignin-related phenolics at alkaline pH. *ACS Catal.* **2017**, *7*, 3454–3465. [[CrossRef](#)]
- Ogola, H.J.O.; Kamiike, T.; Hashimoto, N.; Ashida, H.; Ishikawa, T.; Shibata, H.; Sawa, Y. Molecular characterization of a novel peroxidase from the cyanobacterium *Anabaena* sp. strain PCC 7120. *Appl. Environ. Microbiol.* **2009**, *75*, 7509–7518. [[CrossRef](#)]
- Min, K.; Gong, G.; Woo, H.M.; Kim, Y.; Um, Y. A dye-decolorizing peroxidase from *Bacillus subtilis* exhibiting substrate-dependent optimum temperature for dyes and β-ether lignin dimer. *Sci. Rep.* **2015**, *5*, 1–8.

24. van Bloois, E.; Pazmiño DE, T.; Winter, R.T.; Fraaije, M.W. A robust and extracellular heme-containing peroxidase from *Thermobifida fusca* as prototype of a bacterial peroxidase superfamily. *Appl. Microbiol. Biotechnol.* **2010**, *86*, 1419–1430. [[CrossRef](#)]
25. Rahmanpour, R.; Rea, D.; Jamshidi, S.; Fülöp, V.; Bugg, T.D. Structure of *Thermobifida fusca* DyP-type peroxidase and activity towards Kraft lignin and lignin model compounds. *Arch. Biochem. Biophys.* **2016**, *594*, 54–60. [[CrossRef](#)] [[PubMed](#)]
26. Lončar, N.; Colpa, D.I.; Fraaije, M.W. Exploring the biocatalytic potential of a DyP-type peroxidase by profiling the substrate acceptance of *Thermobifida fusca* DyP peroxidase. *Tetrahedron* **2016**, *72*, 7276–7281. [[CrossRef](#)]
27. Brown, M.E.; Barros, T.; Chang, M.C. Identification and characterization of a multifunctional dye peroxidase from a lignin-reactive bacterium. *ACS Chem. Biol.* **2012**, *7*, 2074–2081. [[CrossRef](#)] [[PubMed](#)]
28. Sainsbury, P.D.; Hardiman, E.M.; Ahmad, M.; Otani, H.; Seghezzi, N.; Eltis, L.D.; Bugg, T.D. Breaking down lignin to high-value chemicals: The conversion of lignocellulose to vanillin in a gene deletion mutant of *Rhodococcus jostii* RHA1. *ACS Chem. Biol.* **2013**, *8*, 2151–2156. [[CrossRef](#)]
29. Roberts, J.N.; Singh, R.; Grigg, J.C.; Murphy, M.E.; Bugg, T.D.; Eltis, L.D. Characterization of dye-decolorizing peroxidases from *Rhodococcus jostii* RHA1. *Biochemistry* **2011**, *50*, 5108–5119. [[CrossRef](#)]
30. Ahmad, M.; Roberts, J.N.; Hardiman, E.M.; Singh, R.; Eltis, L.D.; Bugg, T.D. Identification of DypB from *Rhodococcus jostii* RHA1 as a lignin peroxidase. *Biochemistry* **2011**, *50*, 5096–5107. [[CrossRef](#)]
31. Yu, W.; Liu, W.; Huang, H.; Zheng, F.; Wang, X.; Wu, Y.; Li, K.; Xie, X.; Jin, Y. Application of a novel alkali-tolerant thermostable DyP-type peroxidase from *Saccharomonospora viridis* DSM 43017 in biobleaching of eucalyptus kraft pulp. *PLoS ONE* **2014**, *9*, e110319. [[CrossRef](#)]
32. Li, J.; Liu, C.; Li, B.; Yuan, H.; Yang, J.; Zheng, B. Identification and molecular characterization of a novel DyP-type peroxidase from *Pseudomonas aeruginosa* PKE117. *Appl. Biochem. Biotechnol.* **2012**, *166*, 774–785. [[CrossRef](#)]
33. Rahmanpour, R.; Bugg, T.D. Characterisation of Dyp-type peroxidases from *Pseudomonas fluorescens* Pf-5: Oxidation of Mn (II) and polymeric lignin by Dyp1B. *Arch. Biochem. Biophys.* **2015**, *574*, 93–98. [[CrossRef](#)]
34. Santos, A.; Mendes, S.; Brissos, V.; Martins, L.O. New dye-decolorizing peroxidases from *Bacillus subtilis* and *Pseudomonas putida* MET94: Towards biotechnological applications. *Appl. Microbiol. Biotechnol.* **2014**, *98*, 2053–2065. [[CrossRef](#)] [[PubMed](#)]
35. Létoffé, S.; Heuck, G.; Delepelaire, P.; Lange, N.; Wandersman, C. Bacteria capture iron from heme by keeping tetrapyrrol skeleton intact. *Proc. Natl. Acad. Sci. USA* **2009**, *106*, 11719–11724. [[CrossRef](#)]
36. Tatsumi, N.; Inui, M. (Eds.) *Corynebacterium glutamicum: Biology and Biotechnology*; Springer Science & Business Media: Berlin/Heidelberg, Germany, 2012; Volume 23.
37. Hwang, K.S.; Kim, H.U.; Charusanti, P.; Palsson, B.Ø.; Lee, S.Y. Systems biology and biotechnology of *Streptomyces* species for the production of secondary metabolites. *Biotechnol. Adv.* **2014**, *32*, 255–268. [[CrossRef](#)] [[PubMed](#)]
38. Cappelletti, M.; Presentato, A.; Piacenza, E.; Firrincieli, A.; Turner, R.J.; Zannoni, D. Biotechnology of *Rhodococcus* for the production of valuable compounds. *Appl. Microbiol. Biotechnol.* **2020**, *104*, 8567–8594. [[CrossRef](#)] [[PubMed](#)]
39. Alvarez, H.M.; Mayer, F.; Fabritius, D.; Steinbüchel, A. Formation of intracytoplasmic lipid inclusions by *Rhodococcus opacus* strain PD630. *Arch. Microbiol.* **1996**, *165*, 377–386. [[CrossRef](#)] [[PubMed](#)]
40. Huang, L.; Zhao, L.; Zan, X.; Song, Y.; Ratledge, C. Boosting fatty acid synthesis in *Rhodococcus opacus* PD630 by overexpression of autologous thioesterases. *Biotechnol. Lett.* **2016**, *38*, 999–1008. [[CrossRef](#)]
41. Na, K.S.; Kuroda, A.; Takiguchi, N.; Ikeda, T.; Ohtake, H.; Kato, J. Isolation and characterization of benzene-tolerant *Rhodococcus opacus* strains. *J. Biosci. Bioeng.* **2005**, *99*, 378–382. [[CrossRef](#)]
42. Yamashita, S.; Sato, M.; Iwasa, Y.; Honda, K.; Sameshima, Y.; Omasa, T.; Kato, J.; Ohtake, H. Utilization of hydrophobic bacterium *Rhodococcus opacus* B-4 as whole-cell catalyst in anhydrous organic solvents. *Appl. Microbiol. Biotechnol.* **2007**, *74*, 761–767. [[CrossRef](#)]
43. Tischler, D.; Eulberg, D.; Lakner, S.; Kaschabek, S.R.; van Berkel, W.J.; Schlömann, M. Identification of a novel self-sufficient styrene monooxygenase from *Rhodococcus opacus* 1CP. *J. Bacteriol.* **2009**, *191*, 4996–5009. [[CrossRef](#)]
44. Oelschlägel, M.; Gröning, J.A.; Tischler, D.; Kaschabek, S.R.; Schlömann, M. Styrene oxide isomerase of *Rhodococcus opacus* 1CP, a highly stable and considerably active enzyme. *Appl. Environ. Microbiol.* **2012**, *78*, 4330–4337. [[CrossRef](#)] [[PubMed](#)]
45. Gröning, J.A.; Eulberg, D.; Tischler, D.; Kaschabek, S.R.; Schlömann, M. Gene redundancy of two-component (chloro) phenol hydroxylases in *Rhodococcus opacus* 1CP. *FEMS Microbiol. Lett.* **2014**, *361*, 68–75. [[CrossRef](#)] [[PubMed](#)]
46. Qi, J.; Schlömann, M.; Tischler, D. Biochemical characterization of an azoreductase from *Rhodococcus opacus* 1CP possessing methyl red degradation ability. *J. Mol. Catal. B Enzym.* **2016**, *130*, 9–17. [[CrossRef](#)]
47. Altschul, S.F.; Gish, W.; Miller, W.; Myers, E.W.; Lipman, D.J. Basic local alignment search tool. *J. Mol. Biol.* **1990**, *215*, 403–410. [[CrossRef](#)]
48. Thompson, J.D.; Higgins, D.G.; Gibson, T.J. CLUSTAL W: Improving the sensitivity of progressive multiple sequence alignment through sequence weighting, position-specific gap penalties and weight matrix choice. *Nucleic Acids Res.* **1994**, *22*, 4673–4680. [[CrossRef](#)]
49. Kumar, S.; Stecher, G.; Li, M.; Niyaz, C.; Tamura, K. MEGA X: Molecular evolutionary genetics analysis across computing platforms. *Mol. Biol. Evol.* **2018**, *35*, 1547. [[CrossRef](#)]
50. Shrestha, R.; Huang, G.; Meekins, D.A.; Geisbrecht, B.V.; Li, P. Mechanistic insights into dye-decolorizing peroxidase revealed by solvent isotope and viscosity effects. *ACS Catal.* **2017**, *7*, 6352–6364. [[CrossRef](#)]

51. Graves, P.E.; Henderson, D.P.; Horstman, M.J.; Solomon, B.J.; Olson, J.S. Enhancing stability and expression of recombinant human hemoglobin in *E. coli*: Progress in the development of a recombinant HBOC source. *Biochim. Biophys. Acta (BBA)-Proteins Proteom.* **2008**, *1784*, 1471–1479. [[CrossRef](#)]
52. Sudhamsu, J.; Kabir, M.; Airola, M.V.; Patel, B.A.; Yeh, S.R.; Rousseau, D.L.; Crane, B.R. Co-expression of ferrochelatase allows for complete heme incorporation into recombinant proteins produced in *E. coli*. *Protein Expr. Purif.* **2010**, *73*, 78–82. [[CrossRef](#)] [[PubMed](#)]
53. Smith, A.T.; Santama, N.; Dacey, S.; Edwards, M.; Bray, R.C.; Thorneley, R.N.; Burke, J.F. Expression of a synthetic gene for horseradish peroxidase C in *Escherichia coli* and folding and activation of the recombinant enzyme with Ca<sup>2+</sup> and heme. *J. Biol. Chem.* **1990**, *265*, 13335–13343. [[CrossRef](#)]
54. Kery, V.; Elleder, D.; Kraus, J.P.  $\delta$ -Aminolevulinate increases heme saturation and yield of human cystathionine  $\beta$ -synthase expressed in *Escherichia coli*. *Arch. Biochem. Biophys.* **1995**, *316*, 24–29. [[CrossRef](#)] [[PubMed](#)]
55. Weickert, M.J.; Pagratis, M.; Curry, S.R.; Blackmore, R. Stabilization of apoglobin by low temperature increases yield of soluble recombinant hemoglobin in *Escherichia coli*. *Appl. Environ. Microbiol.* **1997**, *63*, 4313–4320. [[CrossRef](#)] [[PubMed](#)]
56. Varnado, C.L.; Goodwin, D.C. System for the expression of recombinant hemoproteins in *Escherichia coli*. *Protein Expr. Purif.* **2004**, *35*, 76–83. [[CrossRef](#)]
57. Sugano, Y.; Ishii, Y.; Shoda, M. Role of H164 in a unique dye-decolorizing heme peroxidase DyP. *Biochem. Biophys. Res. Commun.* **2004**, *322*, 126–132. [[CrossRef](#)]
58. Chen, C.; Li, T. Bacterial dye-decolorizing peroxidases: Biochemical properties and biotechnological opportunities. *Phys. Sci. Rev.* **2016**, *1*, 1–15. [[CrossRef](#)]
59. Chaplin, A.K.; Chicano, T.M.; Hampshire, B.V.; Wilson, M.T.; Hough, M.A.; Svistunenko, D.A.; Worrall, J.A. An Aromatic Dyad Motif in Dye Decolourising Peroxidases Has Implications for Free Radical Formation and Catalysis. *Chem.—A Eur. J.* **2019**, *25*, 6141–6153. [[CrossRef](#)]
60. Catucci, G.; Valetti, F.; Sadeghi, S.J.; Gilardi, G. Biochemical features of dye-decolorizing peroxidases: Current impact on lignin degradation. *Biotechnol. Appl. Biochem.* **2020**, *67*, 751–759. [[CrossRef](#)]
61. Sugano, Y.; Muramatsu, R.; Ichiyonagi, A.; Sato, T.; Shoda, M. DyP, a unique dye-decolorizing peroxidase, represents a novel heme peroxidase family: ASP171 replaces the distal histidine of classical peroxidases. *J. Biol. Chem.* **2007**, *282*, 36652–36658. [[CrossRef](#)]
62. Sugawara, K.; Nishihashi, Y.; Narioka, T.; Yoshida, T.; Morita, M.; Sugano, Y. Characterization of a novel DyP-type peroxidase from *Streptomyces avermitilis*. *J. Biosci. Bioeng.* **2017**, *123*, 425–430. [[CrossRef](#)] [[PubMed](#)]
63. Wariishi, H.; Gold, M.H. Lignin peroxidases Compound III. *J. Biol. Chem.* **1989**, *265*, 2070–2077. [[CrossRef](#)]
64. de Eugenio, L.L.; Peces-Pérez, R.; Linde, D.; Prieto, A.; Barriuso, J.; Ruiz-Dueñas, F.J.; Martínez, M.J. Characterization of a Dye-Decolorizing Peroxidase from *Irpex lacteus* Expressed in *Escherichia coli*: An Enzyme with Wide Substrate Specificity Able to Transform Lignosulfonates. *J. Fungi* **2021**, *7*, 325. [[CrossRef](#)] [[PubMed](#)]
65. Valderrama, B.; Ayala, M.; Vazquez-Duhalt, R. Suicide inactivation of peroxidases and the challenge of engineering more robust enzymes. *Chem. Biol.* **2002**, *9*, 555–565. [[CrossRef](#)]
66. Liers, C.; Bobeth, C.; Pecyna, M.; Ullrich, R.; Hofrichter, M. DyP-like peroxidases of the jelly fungus *Auricularia auricula-judae* oxidize nonphenolic lignin model compounds and high-redox potential dyes. *Appl. Microbiol. Biotechnol.* **2010**, *85*, 1869–1879. [[CrossRef](#)] [[PubMed](#)]
67. Hoshino, F.; Kajino, T.; Sugiyama, H.; Asami, O.; Takahashi, H. Thermally stable and hydrogen peroxide tolerant manganese peroxidase (MnP) from *Lenzites betulinus*. *FEBS Lett.* **2002**, *530*, 249–252. [[CrossRef](#)]
68. Sugano, Y.; Matsushima, Y.; Tsuchiya, K.; Aoki, H.; Hirai, M.; Shoda, M. Degradation pathway of an anthraquinone dye catalyzed by a unique peroxidase DyP from *Thanatephorus cucumeris* Dec 1. *Biodegradation* **2009**, *20*, 433–440. [[CrossRef](#)] [[PubMed](#)]
69. Lončar, N.; Drašković, N.; Božić, N.; Romero, E.; Simić, S.; Opsenica, I.; Vujčić, Z.; Fraaije, M.W. Expression and Characterization of a Dye-decolorizing Peroxidase from *Pseudomonas fluorescens* Pf0-1. *Catalysts* **2019**, *9*, 463. [[CrossRef](#)]
70. Gorlatov, S.N.; Maltseva, O.V.; Shevchenko, V.I.; Golovleva, L.A. Degradation of chlorophenols by a culture of *Rhodococcus erythropolis*. *Microbiology* **1989**, *58*, 647–651.